Available online at www.sciencedirect.com
ScienceDirect
Ceramics International 35 (2009) 2885–2890
CERAMICS INTERNATIONAL
www.elsevier.com/locate/ceramint

Phase transitional behavior and piezoelectric properties of $BiYbO_3$–$Pb(Ti_{0.5}Zr_{0.5})O_3$–$LiNbO_3$ ceramics

Gao Feng *, Deng Zhenqi, Yang Le, Cheng Lihong, Tian Changsheng

College of Material Science and Engineering, Northwestern Polytechnical University, Xi'an, 710072, China

Received 10 December 2008; received in revised form 10 January 2009; accepted 28 March 2009
Available online 21 May 2009

Abstract

Perovskite $(1-x)(0.06BiYbO_3$–$0.94Pb(Ti_{0.5}Zr_{0.5})O_3)$–$xLiNbO_3$ (BYPTZ-LN) ceramics were synthesized by the conventional ceramic processing. The effect of $LiNbO_3$ on the microstructure and piezoelectric properties was investigated. The perovskite phase and the $Yb_2Ti_2O_7$ pyrochlore phase are coexisting in the BYPTZ-LN ceramics sintered at 1140 °C. The material with perovskite structure is tetragonal at $x \leq 0.04$ and becomes single rhombohedral at $x \geq 0.08$. A morphotropic phase boundary between rhombohedral and tetragonal phases is found in the composition range $0.04 \leq x \leq 0.08$. Analogous to $Pb(Zr,Ti)O_3$, the piezoelectric and electromechanical properties are enhanced for compositions near the morphotropic phase boundary. Piezoelectric constant d_{33} values reach 290–360 pC/N. Electromechanical coefficients k_p reach 0.38–0.55. The maximum values of d_{33}, k_p and P_r are obstained as $x = 0.08$, accompanying with the minimum values of Q_m and E_c. The Curie temperature T_c and the maximum value of dielectric constant decrease with increasing $LiNbO_3$ content. BYPTZ-LN ceramics with the high d_{33} value and the high thermal-depoling temperatures of >320 °C are obtained.
© 2009 Elsevier Ltd and Techna Group S.r.l. All rights reserved.

Keywords: Piezoelectric ceramics; Curie temperature; Pyrochlore phase; C. Electrical properties

1. Introduction

Lead zirconate titanate $Pb(Zr,Ti)O_3$ (PZT) ceramics are the important piezoelectric materials applied and are widely used in electronic sensors, actuators, resonators and filters [1–2]. To improve its piezoelectric properties, most of the researches are focused on adding the complex perovskite type relaxor ferroelectrics. A large number of piezoelectric ceramics are produced with ternary or poly-composition systems such as $Pb(Mn_{1/3}Nb_{2/3})O_3$–$Pb(Zr,Ti)O_3$ [3–4], $Pb(Zn_{1/3}Nb_{2/3})O_3$–$Pb(Zr,Ti)O_3$ [5–6], $Pb(Mg_{1/2}W_{1/2})O_3$–$Pb(Ni_{1/3}Nb_{2/3})O_3$–$Pb(Zr,Ti)O_3$ [7], etc. Nowadays, both the automotive and aerospace industries have expressed the need for actuation and sensing at higher temperatures than currently available. Specifically, under-hood automotive applications such as internal vibration sensors, control surfaces, or active fuel injection nozzles require operation temperatures as high as 300 °C [8]. However, these $Pb(Zr,Ti)O_3$ based ceramics are generally limited to a maximum operating temperature of <200 °C. It is 100 °C lower than the desired operating temperature for applications. So it is necessary to develop high T_c materials with excellent piezoelectric properties.

Over the last few years an increasing amount of research has been done on the development of new piezoelectric materials with a high Curie temperature. These materials involve bismuth-layered structure ferroelectrics and perovskite structure ferroelectric ceramics, such as $CaBi_2Nb_2O_9$ [9], $Pb(Yb_{1/2}Nb_{1/2})O_3$–$PbZrO_3$–$PbTiO_3$ [10], and $BiMeO_3$–$PbTiO_3$ solid solutions (where Me^{3+} = Sc, Ga, In, Fe, etc) [11–15]. In our early research, $BiYbO_3$–$PbTiO_3$ crystalline solutions were fabricated and $BiYbO_3$–$PbTiO_3$ ceramics with high Curie temperatures of >500 °C are obtained. But the problem is that the piezoelectric constant d_{33} is only 28 pC/N [16].

Lithium niobate, $LiNbO_3$, is well known as an important ferroelectric material with the high Curie temperature at 1200 °C. At room temperature, $LiNbO_3$ has a rhombohedral symmetry and space group $R3c$ [17]. $LiNbO_3$ is widely used for $(Na_{0.5}K_{0.5})NbO_3$ based lead-free piezoelectric ceramics to promote piezoelectric properties and the Curie temperature [18–20]. However, the study of $LiNbO_3$ doping on the structure

* Corresponding author.
E-mail address: gaofeng@nwpu.edu.cn (G. Feng).

0272-8842/$36.00 © 2009 Elsevier Ltd and Techna Group S.r.l. All rights reserved.
doi:10.1016/j.ceramint.2009.03.045

and properties of $BiYbO_3$–$Pb(Zr,Ti)O_3$ ceramics has not been reported yet. In this paper, novel $BiYbO_3$–$Pb(Zr,Ti)O_3$ based ceramics have been fabricated as a high Curie temperature piezoelectric. The phase structure and piezoelectric properties of $BiYbO_3$–$Pb(Zr,Ti)O_3$–$LiNbO_3$ are investigated in detail.

2. Experimental

The general formula of the material studied was $(1-x)(0.06BiYbO_3$–$0.94Pb(Ti_{0.5}Zr_{0.5})O_3)$–$xLiNbO_3$ (designated as BYPTZ-LN), where x is 0, 0.02, 0.04, 0.08, and 0.16,respectively. Samples are numbered as BYPTZ-LN_1, BYPTZ-LN_2, BYPTZ-LN_3, BYPTZ-LN_4, and BYPTZ-LN_5 in sequence. Reagent pure Pb_3O_4, Bi_2O_3, TiO_2, ZrO_2, Nb_2O_5, $LiCO_3$ and Yb_2O_3 were used as starting materials. The mixtures were weighed stoichiometrically and ball-milled for 12 h. The powders were pre-calcined at 860 °C for 4 h. After milling for a second time, the powder was pressed into disks 12.0 mm in diameter at 100 MPa, and then sintered at 1140 °C for 2 h. The packing material PbO ZrO_2 was put on to a platinum sheet, and covered with an Al_2O_3 crucible to prevent PbO volatilization. The sintered discs were polished and pasted with silver on both surfaces. Samples were poled at 140 °C for 20 min under an electric field of 3 kV/mm in silicone oil. The piezoelectric properties were measured after 24 h aging at room temperature.

The content of the perovskite phase was examined by X-ray diffraction (XRD, Model Panalytical X'Pert PRO, Holland). For lead-based ferroelectrics, perovskite phase and pyrochlore phase always coexist. The relative amounts of perovskite and pyrochlore phases were determined by measuring the major X-ray peak intensities for perovskite and pyrochlore phases, i.e. (1 0 1) and (2 2 2), respectively. The percentage of perovskite phase was calculated by the following equation [21]:

$$\text{Content of perovskite phase}\,(\%) = \frac{I_{\text{perov}_{(1\,0\,1)}}}{I_{\text{perov}_{(1\,0\,1)}} + I_{\text{pyroc}_{(2\,2\,2)}}} \times 100\% \quad (1)$$

where I_{perov} and I_{pyroc} stand for the intensities of the major peaks (1 0 1) and (2 2 2) for perovskite and pyrochlore phases, respectively. The microstructure was observed by scanning electron microscopy (SEM, Model Hitachi S-570, Japan). The temperature dependence of dielectric constant (ε) and dielectric loss ($tan\ \delta$) were measured between 30 and 550 °C with an LCR precision electric bridge (Model HP4284, Hewlett-Packard). The piezoelectric constant (d_{33}) was measured with a quasistatic piezoelectric d_{33}-meter (Model ZJ-3D, Institute of Acoustics Academic Sinica, China). The electromechanical coupling factor (k_p) and the electromechanical quality factor (Q_m) were determined by the resonance and anti-resonance technique using precise impedance analyzer (Model HP4294A, Hewlett-Packard, CA). The ferroelectric hysteresis loops were observed at room temperature by radiant precision workstation ferroelectric testing system. The samples were submerged in silicone oil to prevent arcing during testing. Thermal-depoling experiments were executed by holding the poled samples for 2 h at various high temperatures, cooling to room temperature, measuring d_{33}, and repeating testing procedure up to 400 °C.

3. Results and discussion

Fig. 1 shows XRD patterns of BYPTZ-LN powders calcined at 860 °C. The perovskite phase is the main phase. With the increasing content of $LiNbO_3$, the diffraction angles of perovskite phase shift to large angles, which reveals that Li^+ and Nb^{5+} solute into perovskite lattice structure. The peaks of original oxide materials such as PbO, and Yb_2O_3 are observed when the content of $LiNbO_3$ is 0.16.

Fig. 2 shows XRD patterns of BYPTZ-LN ceramics sintered at 1140 °C. There are two phases, the perovskite phase and the $Yb_2Ti_2O_7$ pyrochlore phase, coexisting in the BYPTZ-LN ceramics. And the amounts of $Yb_2Ti_2O_7$ pyrochlore phase is stable with the increasing content of $LiNbO_3$. As to $BiYbO_3$–$PbTiO_3$ ceramics, our early research shows that it is difficult to synthesize pure perovskite phase by traditional method [16]. Because the $BiYbO_3$ compound owns a small tolerance factor 0.857, perovskite with such tolerance factor is known to be difficult to synthesise and second phases often appear. It shows that the percentage of the pyrochlore phase is range from 8.19 to 9.76, as listed in Table 1.

What is more, when the content of $LiNbO_3$ is lower than 0.04 mol, it is observed that the double peaks of the perovskite phase appear in the samples, which demonstrates that the perovskite structure exhibits tetragonal symmetry. The tetragonal and rhombohedral structures can be determined from the double peaks at $2\theta \approx 22°$ and $2\theta \approx 45°$. Fig. 3 shows the XRD peaks at 22° and 45°. The intensities of $(0\,0\,1)_T$ and $(0\,0\,2)_T$ increase with the increasing content of $LiNbO_3$. When the content of $LiNbO_3$ is greater than 0.08 mol, the $(0\,0\,1)_T$, $(1\,0\,0)_T$, $(0\,0\,2)_T$ and $(2\,0\,0)_T$ peaks disappear, and only the single $(1\,0\,0)_R$ and $(2\,0\,0)_R$ peak remains. This supports the phase transition from tetragonal to rhombohedral.

When $LiNbO_3$ is added in $0.06BiYbO_3$–$0.94Pb(Ti_{0.5}Zr_{0.5})O_3$ solid solution, the ionic radius of Li^+ (120 pm) [22] is much

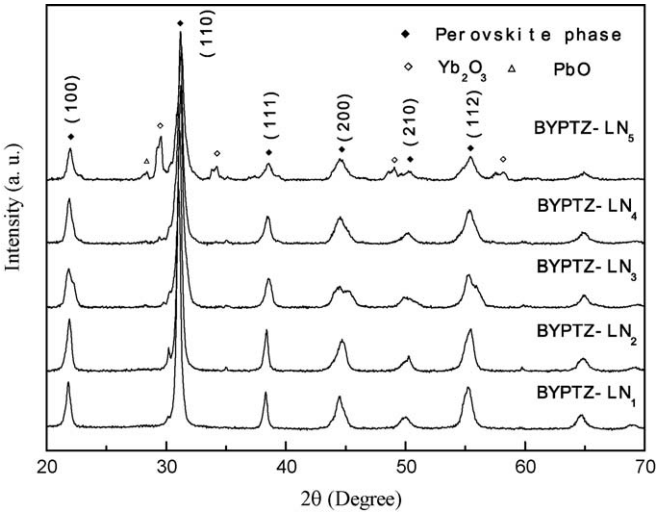

Fig. 1. The XRD patterns of BYPTZ-LN powders calcined at 860 °C.

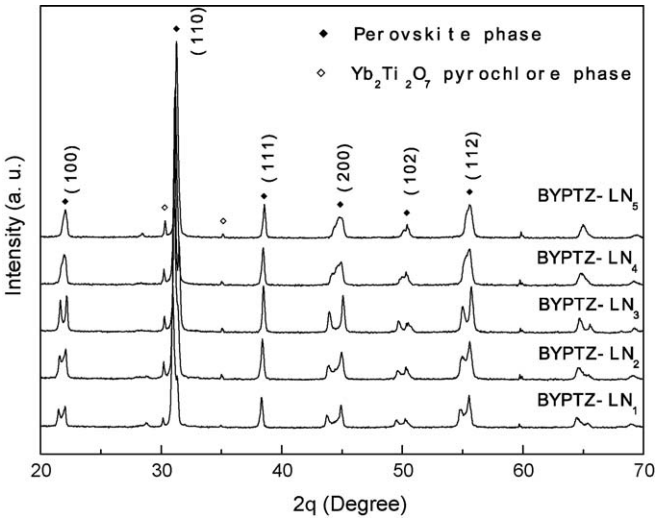

Fig. 2. The XRD patterns of BYPTZ-LN ceramics sintered at 1140 °C.

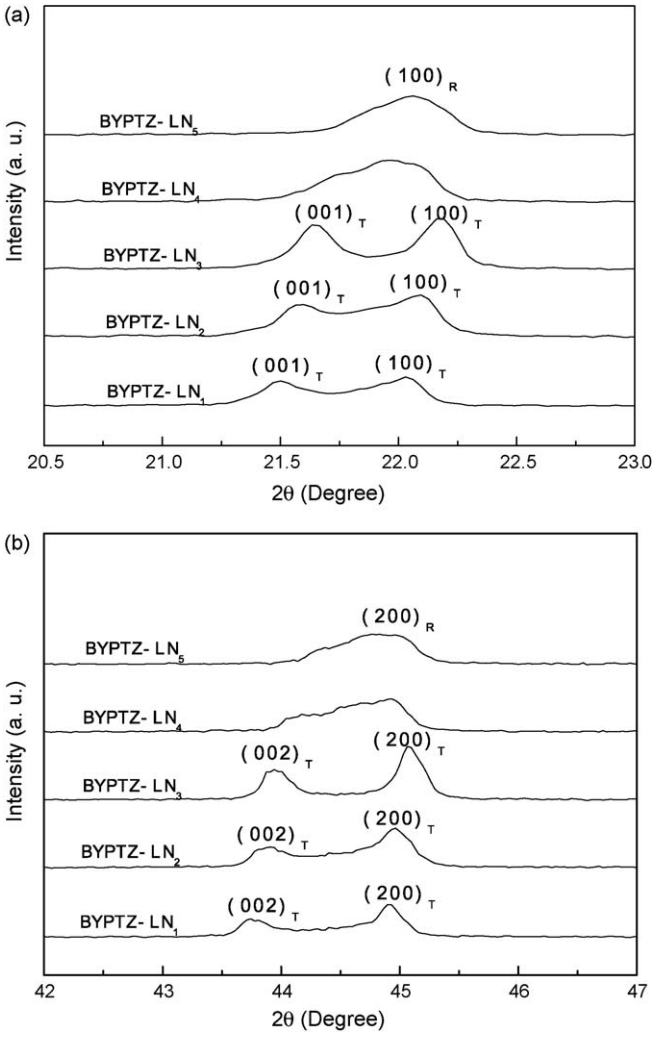

Fig. 3. The XRD patterns at $2\theta \approx 22^\circ$ (a) and $2\theta \approx 45^\circ$ (b) of BYPTZ-LN ceramics.

larger than B-site ion, Ti^{4+} (60.5 pm), Zr^{4+} (74 pm) and Yb^{3+} (86.8 pm), and the valence of Li^+ is smaller than that of Ti^{4+}, Zr^{4+} and Yb^{3+}. Thus Li^+ may easily enter A-site and replace the ions in A-site. Because the ionic radius of Li^+ is smaller than A-site ions, Pb^{2+} (149 pm), and Bi^{3+} (140 pm), which will lead to the distortion of lattice and cause the ferroelectric phase transition. A morphotropic phase boundary (MPB) between rhombohedral and tetragonal phases is found in the composition range $0.04 \leq x \leq 0.08$.

Fig. 4 shows the microstructures of BYPTZ-LN ceramics sintered at 1140 °C. It can be seen that the microstructure of BYPTZ-LN ceramics are uniform and sintered effectively with well-developed grain. An average grain size of 2.03–2.52 μm is observed at $0 \leq x \leq 0.08$ and the fracture is intergranular. With increasing amounts of $LiNbO_3$, the grain size increases. It is well known that the substitutions of $(Ti, Zr)^{4+}$ by Nb^{5+} will lead to the creation of Pb^{2+} vacancies, which can promote the densification and the grain growth of ceramics.

Fig. 5 shows the dielectric properties of BYPTZ-LN ceramics as a function of temperature using a measurement frequency of 1 kHz. For BYPTZ-LN_1 sample, the dielectric constant can be seen to slowly increase with increasing temperature from 30 to 350 °C. Then the dielectric constant increases abruptly as temperature higher than 350 °C, exhibiting a dielectric peak at 385 °C. This transition corresponds to the ferroelectric–paraelectric phase transformation at the Curie temperature. For higher $LiNbO_3$ contents, the dielectric peak shifts to the low temperature and the maximum value of ε reduces from 25421 to 7832. It can be seen that the dielectric loss increases firstly, reaching a plat, and then increasing abruptly. The value of *tan δ* is found to become very large at high temperatures, indicating space charge polarization and associated ionic conductivity.

Fig. 6 shows the variation of the Curie temperature T_c and the piezoelectric constant d_{33} as a function of the content of

Table 1
Phase structure and ferroelectric properties of BYPTZ-LN ceramics.

Samples	BYPTZ-LN_1	BYPTZ-LN_2	BYPTZ-LN_3	BYPTZ-LN_4	BYPTZ-LN_5
Perovskite percentage (%)	91.81	90.24	91.65	91.15	90.61
Pyrochlore percentage (%)	8.19	9.76	8.35	8.85	9.39
Average grain size (μm)	2.03	2.14	2.23	2.52	3.24
ε_{max}	25421	15963	14832	14653	7832
ε	1052	1028	1342	1385	1078
tan δ	0.0244	0.0198	0.0227	0.0297	0.0218
P_r (μC/cm^2)	27.02	25.70	22.11	29.17	19.05
E_c (V/mm)	1597	1613	2380	1555	1609

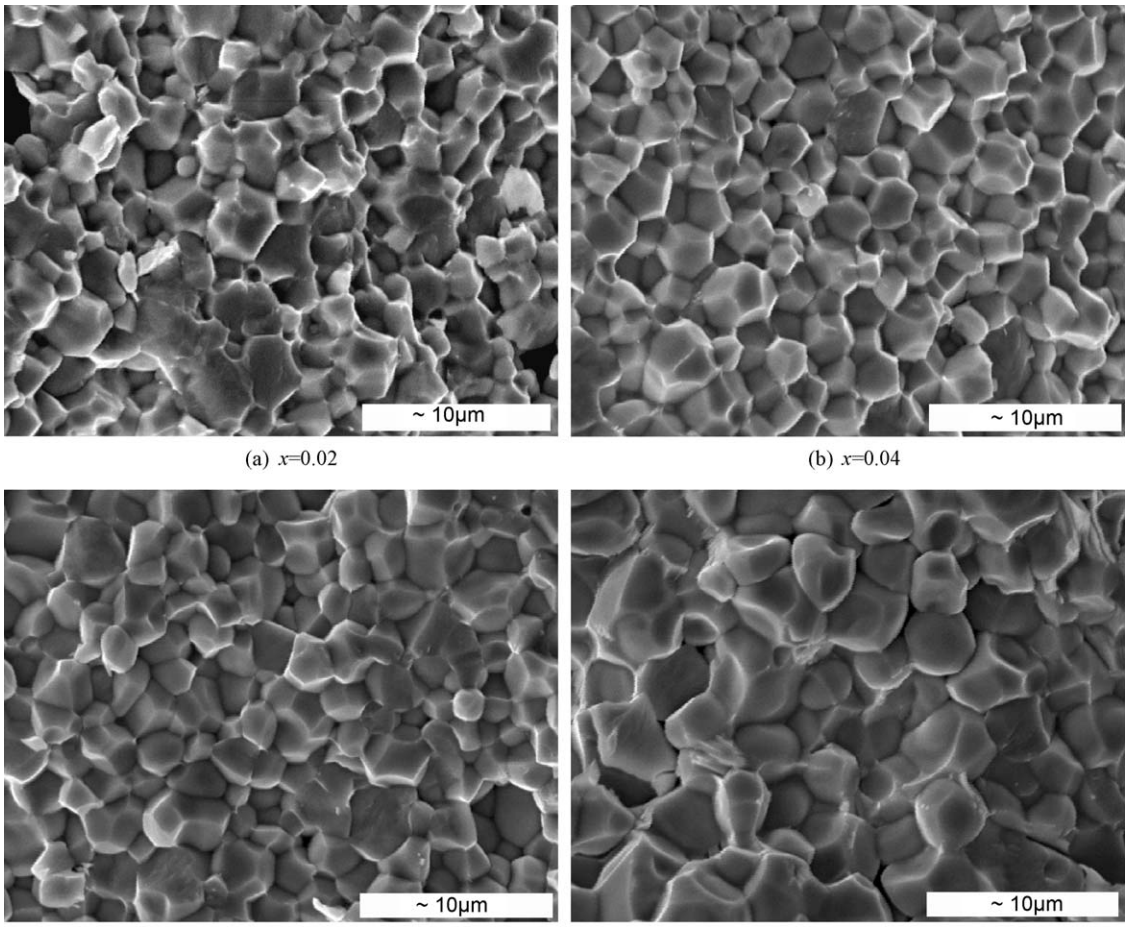

(a) x=0.02 (b) x=0.04

(c) x=0.08 (d) x=0.16

Fig. 4. The SEM photographs of BYPTZ-LN ceramics sintered at 1140 °C.

$LiNbO_3$. As can be seen, the Curie temperature T_c decreases almost lineally from 385 to 270 °C. This classical Vegard behavior implies that the Li^+ and Nb^{5+} ions are being diffused into the ABO_3 perovskite structure and occupied the A-sites and B-sites, respectively. The reduction in T_c with $LiNbO_3$ substitution is ~9.6 °C/mol% $LiNbO_3$, which is similar to the results observed by Chen et al. [23]. That the addition of $LiNbO_3$ did not result in higher T_c in the BYPTZ-LN system should be attributed to the structural transition from tetragonal to rhombohedral symmetry with increasing $LiNbO_3$ content, as other MPB systems, of which the tetragonal side generally has higher T_c than the rhombohedral-side [23].

It can be found that d_{33} increases from 255 to 360 pC/N with increasing amounts of $LiNbO_3$. The maximum value of d_{33} is obtained as $x = 0.08$. However, with the further increasing of $LiNbO_3$ content, d_{33} of the composition $x = 0.16$ deteriorates seriously to 200 pC/N. The deteriorate of d_{33} indicates that quite a few of Li^+ ions do not take up the A-sites for $x = 0.16$, because the solubility of Li^+ at higher $LiNbO_3$ concentrations into A-sites becomes more difficult in BYPTZ-LN ceramics with rhombohedral symmetry. It is well known that traditional $Pb(Zr_{1-x}Ti_x)O_3$ ceramics lie near the morphotropic phase boundary (MPB) and exhibit anomalously high dielectric and piezoelectric properties. It is concluded that the MPB of BYPTZ-LN ceramics lies in the composition range $0.04 \leq x \leq 0.08$.

Fig. 7 shows the relationship between the electromechanical coupling factor (k_p) and the mechanical quality factor (Q_m) as a function of $LiNbO_3$ content. k_p and Q_m change the opposite sense with different amounts of $LiNbO_3$. Firstly Q_m increases when the content of $LiNbO_3$ increases. The maximum value of 1043 appears at $x = 0.04$. After that, Q_m decreases to the minimum value of 284 obtained at $x = 0.08$. In contrast, k_p first decreases with the minimum value of 0.38 obtained at $x = 0.04$, then k_p increases with increasing $LiNbO_3$ content. The maximum value of k_p amounts to 0.55 at $x = 0.08$.

Fig. 8 shows the hysteresis loops of BYPTZ-LN ceramics. The shape of hysteresis loop changes regularly. The remnant polarization P_r decreases and the coercive field E_c increases obviously with the increasing amount of $LiNbO_3$. As Table 1 shows, for the BYPTZ-LN_1 sample, E_c is 1597 V/mm, P_r is 27.02 μC/cm^2. But for the BYPTZ-LN_3 sample, P_r decreases to 22.11 μC/cm^2 and E_c increases to 2380 V/mm. What is more, the E_c and P_r of BYPTZ-LN_4 sample show much difference with other samples. The maximum value of P_r (29.17 μC/cm^2) and the minimum value E_c (1555 V/mm) are obtained at $x = 0.08$. All of the piezoelectric properties have an inflexion at $x = 0.08$ mol.

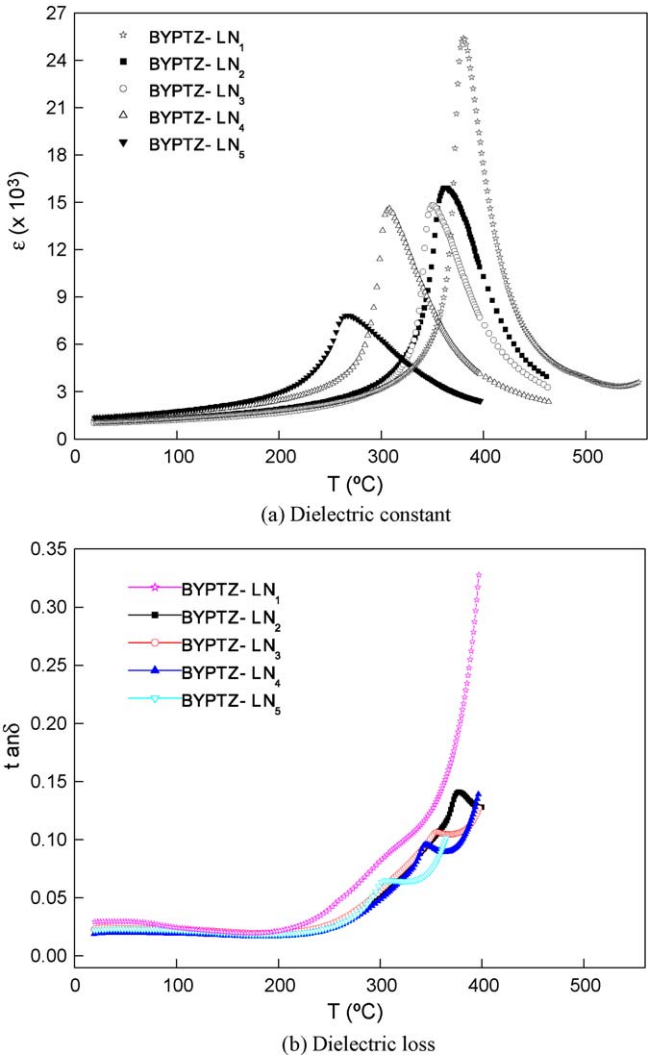

Fig. 5. The dielectric properties as a function of temperature for BYPTZ-LN ceramics (1 kHz).

In addition to measurements at room temperature, the piezoelectric activity was also studied as a function of temperature. The thermal-depoling behavior of the BYPTZ-LN samples was shown in Fig. 9, in which piezoelectric constant d_{33} are plotted against the annealing temperature. The d_{33} values of the BYPTZ-LN_1, BYPTZ-LN_2, and BYPTZ-LN_3 samples were stable up to 300 °C, and dropped rapidly above 320 °C, while the sample was fully depoled at >370 °C. The d_{33} values of the BYPTZ-LN_4, and BYPTZ-LN_5 samples were stable up to 125 °C, above which these samples lost piezoelectric activity. They were fully depoled at temperatures between 270 and 300 °C. The results demonstrates that the tetragonal phase shows the higher depoling temperature than rhombohedral phase for BYPTZ-LN ceramics.

For the traditional applications, BYPTZ-LN_4 samples lies in the MPB and exhibits excellent piezoelectric properties with $d_{33} = 360$ pC/N and $k_p = 0.55$. But for high-temperature piezoelectric applications, BYPTZ-LN_3 ceramics with the high thermal-depoling temperature (up to 320 °C) is a promising material shown the optimized piezoelectric properties of $T_c = 350$ °C, $d_{33} = 290$ pC/N and $Q_m = 1043$.

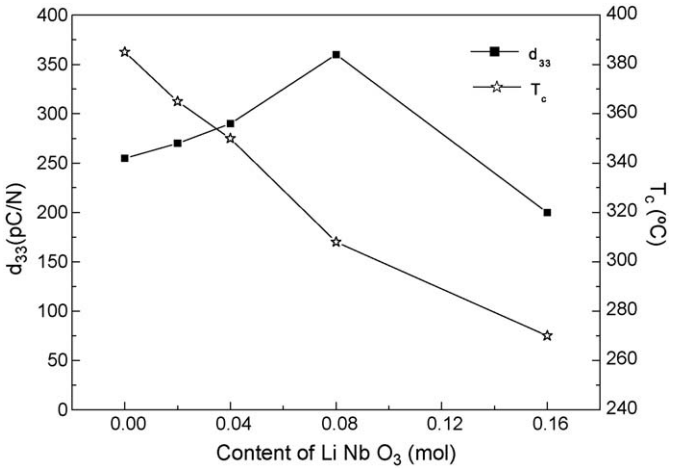

Fig. 6. The piezoelectric coefficient d_{33} and Curie temperature T_c of BYPTZ-LN ceramics.

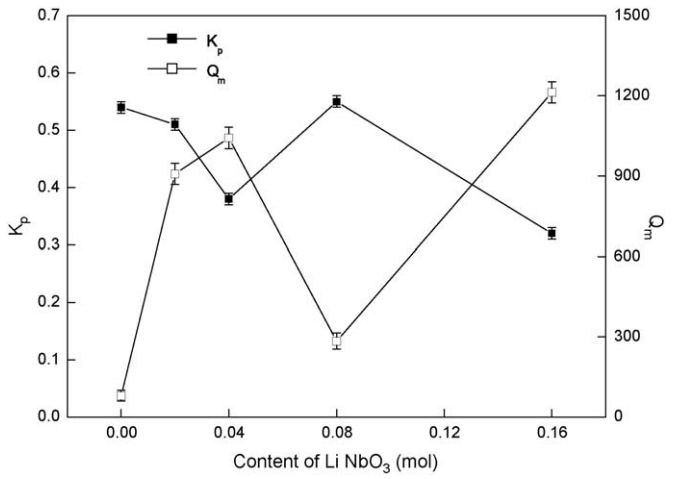

Fig. 7. The k_p and Q_m of BYPTZ-LN ceramics with different amounts of $LiNbO_3$.

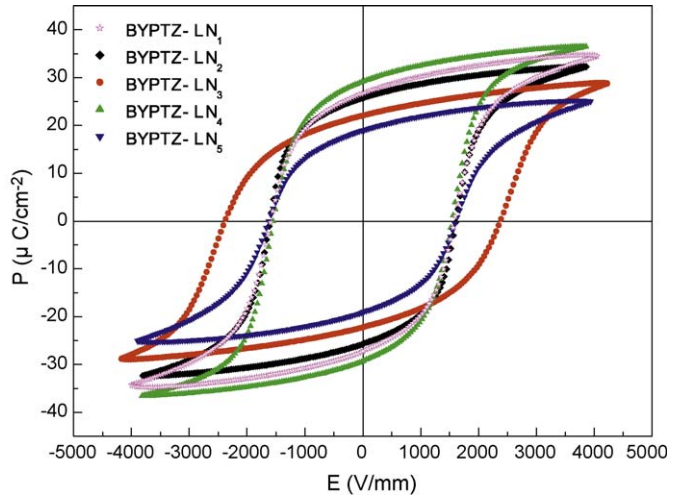

Fig. 8. Hysteresis loops of BYPTZ-LN ceramics with different amounts of $LiNbO_3$.

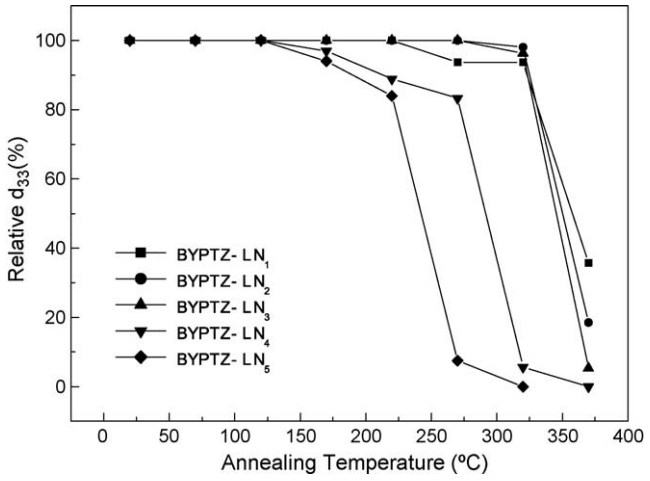

Fig. 9. The annealing temperature and the relative d_{33} of BYPTZ-LN ceramics.

4. Conclusions

Perovskite BYPTZ-LN ceramics were prepared by the conventional ceramic processing. The perovskite phase and the $Yb_2Ti_2O_7$ pyrochlore phase are coexisting in the BYPTZ-LN ceramics. The substitution of $LiNbO_3$ makes the crystalline symmetry of BYPTZ-LN perovskite structure change from the tetragonal to the rhombohedral, and the tetragonal and rhombohedral phases coexist in a broad composition range $0.04 \leq x \leq 0.08$, in which the ceramics exhibit excellent piezoelectric properties. The maximum electromechanical values of $d_{33} = 360$ pC/N and $k_p = 0.55$ were gained in BYPTZ-LN_4 for $x = 0.08$, as well as the highest remnant polarization $P_r = 29.17$ μC/cm^2. But the Curie temperature T_c decreases from 385 to 270 °C and the maximum value of dielectric constant decreases from 25421 to 7832 with the increasing content of $LiNbO_3$. BYPTZ-LN_4 ceramics with excellent piezoelectric properties can be used in the normal applications, and BYPTZ-LN_3 ceramics by a combination of high T_c (350 °C), high Q_m (1043), stable d_{33}, and high thermal-depoling temperature is a very promising material used for high-temperature (up to 320 °C) applications.

Acknowledgments

This work was supported by Natural Science Foundation of Shanxi Province in China, Science and Technology Innovation Fund of Northwestern Polytechnical University and Outstanding Scholars Fund of Northwestern Polytechnical University.

References

[1] M. Kenji, D. Mabuchi, K. Takahiro, et al., Effects of adding various metal oxides on low-temperature sintered Pb(Zr, Ti)O_3 ceramics, Jpn. J. Appl. Phys. 35 (9B) (1996) 5188–5191.

[2] Y.D. Hou, M.K. Zhu, H. Wang, et al., Piezoelectric properties of new MnO_2-added 0.2PZN–0.8PZT ceramics, Mater. Lett. 58 (2004) 1508–1512.

[3] B. Li, G. Li, W. Zhang, et al., Influence of particle size on the sintering behavior and high-power piezoelectric properties of PMnN–PZT ceramics, Mater. Sci. Eng. B 121 (2005) 92–97.

[4] C.Y. Chen, Y. Hu, H.L. Lin, et al., Influence of the sintering temperature on phase development in PMnN–PZT ceramics, Ceram. Int. 33 (2007) 263–268.

[5] G. Feng, W. Chunjuan, L. Xiangchun, et al., Effect of tungsten on the structure and piezoelectric properties of PZN–PZT ceramics, Ceram. Int. 33 (6) (2007) 1019–1023.

[6] Y.D. Hou, M.K. Zhu, H. Wang, et al., Effects of CuO addition on the structure and electrical properties of low temperature sintered Pb$((Zn_{1/3}Nb_{2/3})_{0.20}(Zr_{0.50}Ti_{0.50})_{0.80})O_3$ ceramics, Mater. Sci. Eng. B 110 (2004) 27–31.

[7] J.Y. Ha, J.W. Choi, C.Y. Kang, et al., Effects of ZnO on piezoelectric properties of 0.01PMW–0.41PNN–0.35PT–0.23PZ ceramics, Mater. Chem. Phys. 90 (2005) 396–400.

[8] S. Chen, X. Dong, C. Mao, et al., Thermal stability of $(1-x)BiScO_3$–$xPbTiO_3$ piezoelectric ceramics for high-temperature sensor applications, J. Am. Ceram. Soc. 89 (10) (2006) 3270–3272.

[9] H. Yan, H. Zhang, R. Ubic, et al., A lead-free high-curie-point ferroelectric ceramic $CaBi_2Nb_2O_9$, Adv. Mater. 17 (2005) 1261–1265.

[10] W.M. Zhu, Z.G. Ye, Ternary Pb$(Yb_{1/2}Nb_{1/2})O_3$–$PbZrO_3$–$PbTiO_3$ system as high-T_c/high-piezoelectric materials, Ceram. Int. 30 (2004) 1443–1448.

[11] R.E. Eitel, C.A. Randall, T.R. Shrout, et al., New high temperature morphotropic phase boundary piezoelectrics based on Bi(Me)O_3–$PbTiO_3$ ceramics, Jpn. J. Appl. Phys. 40 (2001) 5999–6002.

[12] R.E. Eitel, S.J. Zhang, T.R. Shrout, et al., Phase diagram of the perovskite system $(1-x)BiScO_3$–$xPbTiO_3$, J. Appl. Phys. 96 (5) (2004) 2828–2831.

[13] R. Duan, R.F. Speyer, E. Alberta, et al., High curie temperature perovskite $BiInO_3$–$xPbTiO_3$ ceramics, J. Mater. Res. 19 (7) (2004) 2185–2192.

[14] J.R. Cheng, W. Zhu, N. Li, et al., Fabrication and characterization of $xBiGaO_3$–$(1-x)PbTiO_3$: a high temperature reduced Pb-content piezoelectric ceramic, Mater. Lett. 57 (2003) 2090–2094.

[15] P. Comyn, S.P. McBride, A.J. Bell, Processing and electrical properties of $BiFeO_3$–$PbTiO_3$ ceramics, Mater. Lett. 58 (2004) 3844–3846.

[16] G. Feng, H. Rongzi, L. Jiaji, et al., Phase formation and characterization of high Curie temperature $xBiYbO_3$–$(1-x)PbTiO_3$ piezoelectric ceramics, J. Europ. Ceram. Soc. 29 (2009) 1687–1693.

[17] A.Z. Simoes, A.H.M. Gonzalez, A.A. Cavalheiro, et al., Effect of magnesium on structure and properties of $LiNbO_3$ prepared from polymeric precursors, Ceram. Int. 28 (2002) 265–270.

[18] Y. Guo, K. Kakimoto, H. Ohsato, Phase transitional behavior and piezoelectric properties of $Na_{0.5}K_{0.5}NbO_3$–$LiNbO_3$ ceramics, Appl. Phys. Lett. 85 (18) (2004) 4121–4123.

[19] F. Tang, H. Du, Z. Li, et al., Preparation and properties of $(Na_{0.5}K_{0.5})NbO_3$–$LiNbO_3$ ceramics, Trans. Nonferr. Met. Soc. 16 (2006) 466–469.

[20] N.M. Hagh, B. Jadidian, A. Safari, Property-processing relationship in lead-free (K, Na, Li) NbO_3-solid solution system, J. Electroceram. 18 (2007) 339–346.

[21] J.R. Belsick, A. Halliyal, U. Kumar, et al., Phase relations and dielectric properties of ceramics in the system Pb$(Zn_{1/3}Nb_{2/3})O_3$–$SrTiO_3$–$PbTiO_3$, Am. Ceram. Soc. Bull. 66 (4) (1987) 664–667.

[22] Y. Yamashita, Y. Hosono, K. Harada, et al., Effect of molecular mass of B-site ions on electromechanical coupling factors of lead-based perovskite piezoelectric materials, Jpn. J. Appl. Phys. 39 (2000) 5593–5596.

[23] Y. Chen, J. Zhu, D. Xiao, et al., Structural and piezoelectric properties of $LiNbO_3$-modified $BiScO_3$–$PbTiO_3$ ceramics, J. Alloys Compd. 470 (1–2) (2009) 420–423.